A short-lived aeolian event during the Early Holocene in southeastern Norway

Helena Alexanderson[a,*] & Mona Henriksen[b]

[a]Department of Geology, Lund University, Sölvegatan 12, SE-223 62 Lund, Sweden; helena.alexanderson@geol.lu.se

[b]Department of Environmental Sciences, Norwegian University of Life Sciences, PO Box 5003, NO-1432 Ås, Norway; mona.henriksen@nmbu.no

*Corresponding author. Phone: +46-462224483

The Starmoen dune field is part of a larger aeolian system in the Jømna and Glomma river valleys in southeastern Norway. It is believed to have formed just after the last deglaciation in the area, but no absolute ages have been available to support this. Here, we present a set of quartz optically stimulated luminescence (OSL) ages from the aeolian sediments and the underlying glacifluvial deposits. The results show that the main dune-building phase was a short-lived event ~10 ka ago, likely with a duration less than a few hundred years. This suggests a rapid stabilisation of an initially unstable environment in newly deglaciated terrain. A much younger event with limited and surficial reworking of sand is dated to 770±110 years ago, and the modern age of an active dune provide additional OSL quality control. Age overestimation is found for glacifluvial sediments, probably due to incomplete bleaching as indicated by e.g. scattered dose distributions from small aliquots. OSL measurements were conducted using coarse quartz grains (180-250 um), which show a dominance of a fast signal component.

Keywords: OSL, eolian, inland dune, Holocene, Norway

1. Introduction

Aeolian deposits can provide much palaeoenvironmental information (e.g. Wolfe, 2007), but in Fennoscandia, with Denmark as an exception, this record in the form of e.g. inland dune fields and cover sands is largely underused and above all, poorly constrained in age (Klemsdal, 1969; Seppälä, 1972; Bergqvist, 1981). Most inland dunes are believed to have formed right after the last

deglaciation, with Holocene reactivation occurring in some areas, but few absolute ages have been reported to support this (e.g. Lundqvist and Mejdahl, 1995; Käyhkö et al., 1999; Alexanderson and Fabel, 2015). Windblown sediments are usually ideal material for OSL dating (Bateman, 2008; Lancaster, 2008), but extensive application to aeolian deposits in Sweden, Norway and Finland is so far relatively limited. This work is part of a larger project that focusses on the inland aeolian record in south-central Sweden and Norway, to establish its chronology and explore its palaeoenvironmental significance. The main objective of this study is to provide a chronological framework for the Starmoen dune field, one of Norway's largest fossil dune fields (Klemsdal, 2010), and to determine its relationship to deglacial events and its Holocene history.

2. Setting

The study area is located in the Jømna valley in SE Norway, ca. 6 km east of the town Elverum and 117 km northeast of Oslo (Fig. 1). The Jømna valley is a c. 13 km long broad side valley of the Glomma River valley, to which it is connected both at its northern and southern ends. Surrounding the valleys are hills reaching 300-500 m a.s.l.

The sediment cover is in general thick with till deposits on the hilly areas, and fluvial, glacifluvial and aeolian sediment in the valleys, where the latter two deposits are believed to have formed at or just after the last deglaciation of the area (Bargel, 1983). At that time ice remnants filled much of the valleys and running water along the western side of the Jømna valley deposited a kame-terrace at 220-200 m a.s.l., ca. 30 m above the present level of Glomma River (Bargel, 1983) (Fig. 1). The glacifluvial material consists mainly of horizontal to gently sloping beds of medium and fine sand but also of gravel beds and scattered cobbles and boulders (Bargel, 1983). As the glacier withdrew from the area, and consequently the inflow of meltwater ceased, it is believed that the glacifluvial sand was exposed to wind, leading to the formation of aeolian dunes (Holtedahl, 1953; Bargel, 1983). Although the deglaciation of the area is not dated, the ice margin was located close to Elverum when an ice-dammed lake broke through the remaining Scandinavian Ice Sheet and caused a large flood (jökulhlaup) that deposited a wide-reaching silt layer, found between 30 to 200 km south and southwest of Elverum (Longva and Thoresen, 1991). This flood layer is associated with the more proximal and coarser sandy deposits along the Glomma valley, including the glacifluvial sand in the Jømna valley, and a boulder deposit 4 km north of Elverum (Longva, 1994). The silt layer is dated c. 80 km further southwest to between 10.5-9.9 cal. ka BP (9045±105 BP below the silt) and 11.2-9.7 cal. ka BP (9230±290 BP above the silt; Longva, 1994), i.e. ~10.5-10 cal. ka BP.

The Starmoen dune field (60.9°N, 11.7°E) is located in the western part of the Jømna valley (Fig. 1) and overlies glacifluvial deposits. It is part of a larger system of aeolian landforms in this area. It

consists of crescentic to parabolic dune ridges, dune heaps and interdune sandsheets, and the dunes are up to 250-300 m long, 20-50 m wide and 2-6 m high (Klemsdal, 2010). The direction of the dune-ridge crests are mainly east-west, slightly concave towards the north (Fig. 1). A forest fire in 1976 covered large parts of the Starmoen dune field (Klemsdal, 2010); it destroyed ca. 9 km^2 of vegetation and caused some reactivation of the aeolian sand.

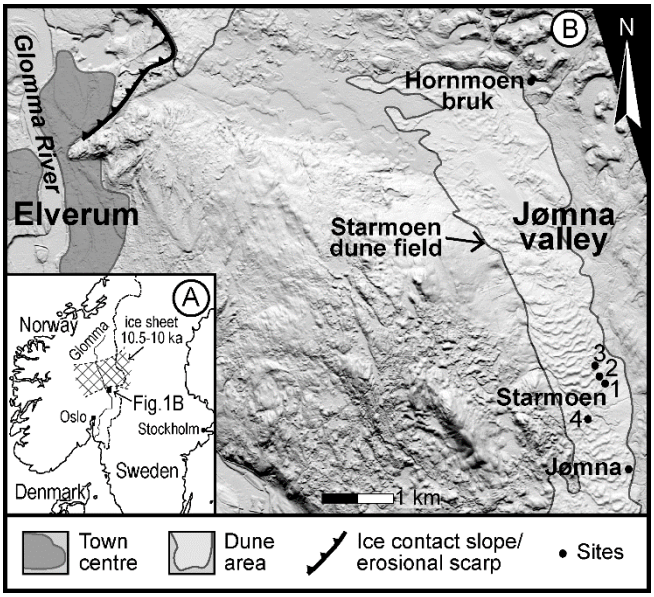

Fig. 1. A. Location of the study area (small square) and the Glomma River in southeastern Norway. The outline of the remaining Scandinavian Ice Sheet in SE Norway at c. 10.5-10 ka is according to Longva (1994). B. Hill-shade model of the Starmoen dune field located close to Elverum. Our sites form a transect from the north to the south in the middle part of the Jømna valley.

The investigated sites (Figs. 1, 2) are documented by detailed sedimentological logging and ground-penetrating radar, the results of which are presented elsewhere (Henriksen et al., in prep.). In general, the dunes consist of low-angle dune foresets covered by superimposed small dunes and/or bioturbated sand sheets (Fig. 2). The grain size is chiefly fine sand similar to the underlying glacifluvial channel deposits; although the latter also contains coarse sand and gravel beds. At the edge of a sand pit (Starmoen 2), small 50-60 cm high aeolian dunes are partly covering young trees around 6 years old, showing that these dunes are presently active. Two soil layers interbedded by a sand layer (c. 10 cm in thickness) were found at Starmoen 4, located in the area affected by the forest fire in 1976. The upper soil layer is very thin (<5 cm, Fig. 2).

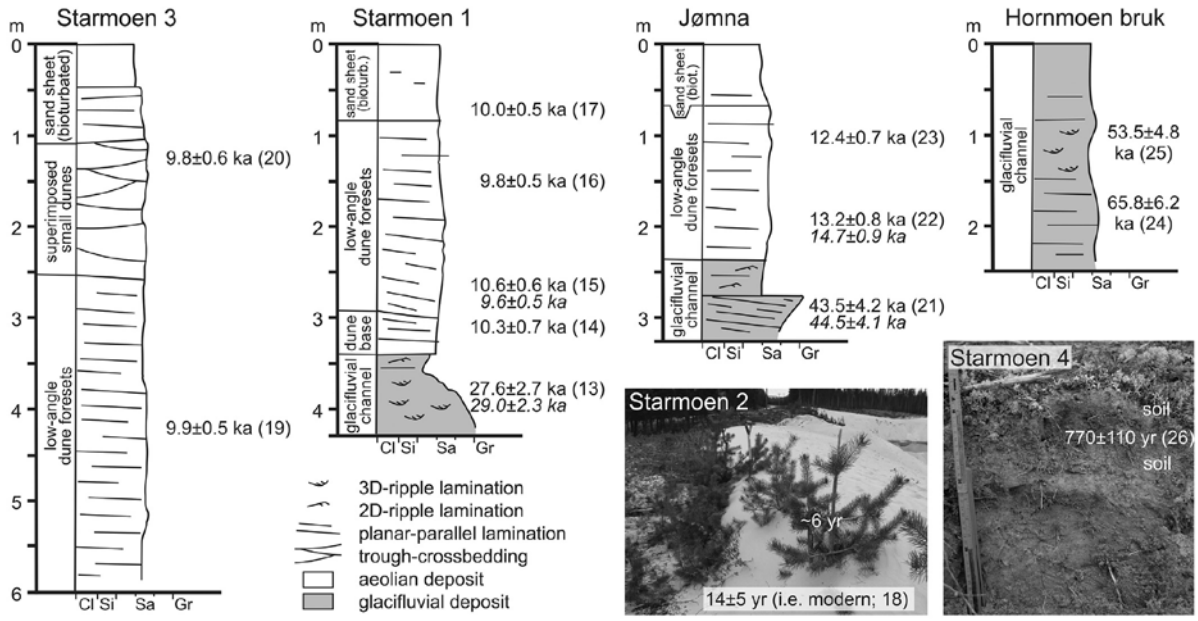

Fig. 2. Simplified logs, photos and OSL ages from the sites at Starmoen, Jømna and Hornmoen bruk. Note that the ages in italics are determined from small aliquots, see Table S1 for full OSL dataset where also Minimum age model (MAM-3) ages are presented. The last two digits of the sample ID are given in parenthesis after the age.

3. Luminescence dating

Fourteen samples for luminescence dating (Table S1) were taken during fieldwork in May 2013. They were analysed at the Lund Luminescence Laboratory at Lund University, Sweden. The environmental dose rate was determined by high-resolution gamma spectrometry (Murray et al., 1987) at the Nordic Laboratory for Luminescence Dating in Denmark and by considering the contribution from cosmic radiation according to Prescott and Hutton (1994).

OSL measurements were conducted using large (8 mm; all samples) and small (2 mm; four samples) aliquots of 180-250 µm quartz grains with a Risø TL/OSL reader model DA-20. SAR-protocols (Murray and Wintle, 2000, 2003; Banerjee et al., 2001) were adapted for each sample based on IR-tests (Duller, 2003), dose recovery analysis and preheat plateau tests and selected preheat temperatures are from 180° to 260° (Table S2, Fig. S3). The apparent dose of bleached samples measured at 260° preheat is 0.4±0.1 Gy, i.e. ~1% of the typical D_e for the samples heated to this temperature before measurement, and is considered insignificant.

The signal from the analysed quartz is dominated by a fast component and the luminescence response rises steadily with dose (Fig. S4). The mean dose recovery ratio is 1.01±0.02 (n=38), which shows that our selected protocols are able to reproduce known given doses. The mean recycling ratio is 1.002±0.004 (n=344) and recuperation <1%. Aliquots were accepted if recycling ratio was within 10% of unity, test dose error <10% and the signal more than three standard deviations above the

background. Any aliquots with infrared/blue ratio >10% were also rejected. OSL sensitivity was calculated in counts·s^{-1}·Gy^{-1} from the response to the first test dose of large aliquots containing roughly the same amount of grains. For the young samples, only those aliquots that had a clear peak in their decay curves were included in sensitivity calculations. D_e(t)-plots (Bailey, 2003) were calculated for six samples by integrating 0.32 s (two channels) at successively longer stimulation times and subtracting a background (last 32 s).

For the small-aliquot data, the single-aliquot decision protocol of Arnold et al. (2007) was followed and the three-parameter minimum-age model (MAM-3; Galbraith et al., 1999) was applied to the data by using an excel macro constructed by Sebastien Huot. Before calculations, an additional error of 10%, based on the overdispersion of dose-recovery results (8±2%), was added to each value.

For further details on methods, see Supplementary materials.

4. Results

The determined D_e values range from 0.05 to 200 Gy and the total dose rates from 2.16 to 3.62 Gy/ka (Tables S1, S5). The glacifluvial deposits have mean OSL ages of 66-28 ka and minimum-age model (MAM-3) ages of 23-14 ka (Fig. 2, Table S1). The dunes at Starmoen are 11-10 ka old, while the dune at Jømna appears slightly older (13-12 ka). The sand between the two soils at Starmoen 4 is 770±110 years old and the active cliff-top dune at Starmoen 2 has an age of 14±5 years (Fig. 2, Table S1). All small-aliquot dose distributions are positively skewed, however, only glacifluvial sample 13021 is significantly skewed (Fig. 3, S6). Apart from aeolian sample 13015, the distributions are also broad, with relative standard deviations of 23-45% (overdispersion 16-37%). D_e(t) plots show rising trends in D_e with stimulation time for glacifluvial sediments, and largely horisontal but slightly rising trends for aeolian sediments (Fig. S7).

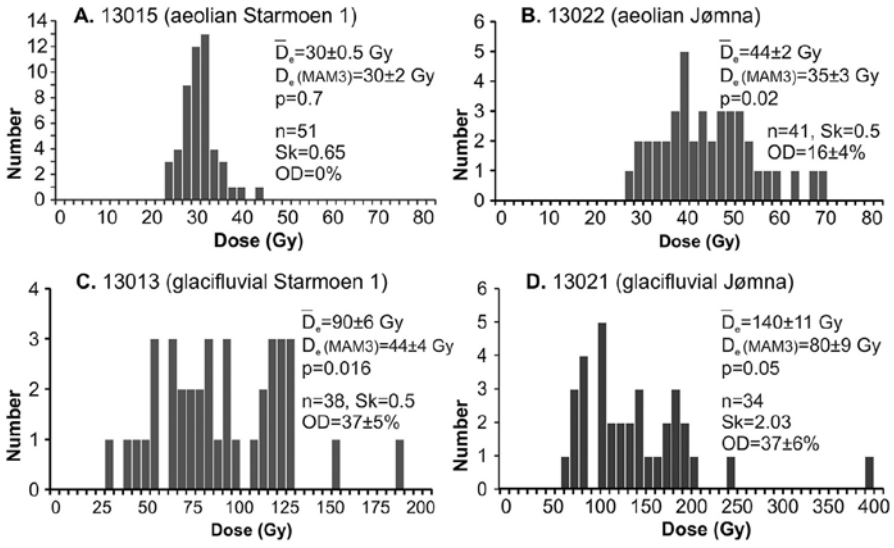

Fig. 3. Dose distributions from small aliquots of two aeolian and two glacifluvial samples from the sites Starmoen 1 and Jømna. A. Lund-13015 from aeolian sand, B. Lund-13022 from aeolian sand, C. Lund-13013 from glacifluvial sand and D. Lund-13021 from glacifluvial sand.

5. Discussion

5.1. Luminescence characteristics

The dose distribution of the Starmoen aeolian sample (Fig. 3A, S6A) is narrow and largely symmetric, as has been shown for other aeolian deposits (Olley et al., 1998; Lepper et al., 2000); the one from Jømna (13021; Fig. 3B, S6B) is much broader. Broad dose distributions in aeolian sediments have been found in other studies, and have been attributed to instrumental error, intrinsic luminescence properties, differential bleaching, microdosimetry or post-depositional mixing (e.g. Vandenberghe et al., 2003; Lomax et al., 2007). In this case, we can rule out instrumental error since the effect seems to be site specific, and samples from different sites have been measured interchangeably. This suggests that the cause is some difference in material characteristics or depositional history. Luminescence characteristics do not seem to be able to account for the difference in dose distribution scatter, but sedimentological differences between the sites (Henriksen et al., in prep.) suggest that more variable sedimentological processes at Jømna may be the cause of the broad dose distributions.

The two small-aliquot dose distributions from glacifluvial sediments are broader than the aeolian ones, and the distribution from sample 13021 is significantly skewed, with a tail of high doses (Fig. 3, S6). This suggests that incomplete bleaching took place and that the age overestimates the true age, which is not unusual for glacifluvial sediments (Thrasher et al., 2009; Alexanderson and Murray, 2012), see discussion of chronological implications below.

It has been shown empirically that luminescence sensitivity depends on the sediment history of the quartz grains and tends to increase with increasing transport distance and the number of erosional-depositional (bleaching-dosing) cycles a grain has undergone (Pietsch et al., 2008; Fitzsimmons, 2011; Jeong and Choi, 2012). Based on sedimentological evidence, Henriksen et al. (in prep.; also Alexanderson & Henriksen 2014) show that the impact of aeolian reworking on the glacifluvial source sediments at Starmoen was very slight and, correspondingly, we see no significant difference in sensitivity between glacifluvial (174-944 counts·s^{-1}·Gy^{-1}) and deglacial-age aeolian sediments (104-593 counts·s^{-1}·Gy^{-1}). The sensitivity is fairly low, which is typical for glacifluvial sediments, especially those derived from magmatic or metamorphic rocks (Thrasher et al., 2009; Alexanderson and Murray, 2012). However, the two young aeolian samples (13018, 13026) have higher luminescence sensitivity (1400-2300 counts·s^{-1}·Gy^{-1}; Table S1), suggesting that the recent

reworking may have had a larger impact on the luminescence characteristics. To resolve this further, detailed investigations, preferably at single-grain level, are needed.

5.2. Timing of deglaciation

The OSL ages of the glacifluvial deposits (66-28 ka; Table S1) are at face value not deglacial, but interstadial. However, there are several indications of that the ages are overestimated due to incomplete bleaching. The glacifluvial sediments have been interpreted to represent one event (the last deglaciation) (Bargel, 1983) and from a geological point of view it is unlikely that the sediments represent such a large span of ages (Henriksen et al., in prep.). OSL data support this, as the ages do not fall on a line in the D_e-dose rate plot (Fig. 4), suggesting some other underlying factor for the measured dose than linear accumulation according to the current dose rate. In addition, D_e(t)-plots (Bailey, 2003) shows a rising trend (Fig. S6) and, as mentioned above, the dose distributions are wide and/or skewed (Fig. 3). The calculated MAM-3 ages are younger but still disparate (23-14 ka; Table S1), and the low p-values show that they are not reliable. Our OSL ages thus only provide a maximum age estimation (28±3 ka) of the deposition of the glacifluvial sediments. A more constraining, although not local, age is provided by the date of the jökulhlaup in the main valley (~10.5-10 cal. ka BP; Longva, 1994), since this must have been contemporaneous – within dating resolution – with the deposition of the meltwater sediments in the Jømna valley (see 2 above).

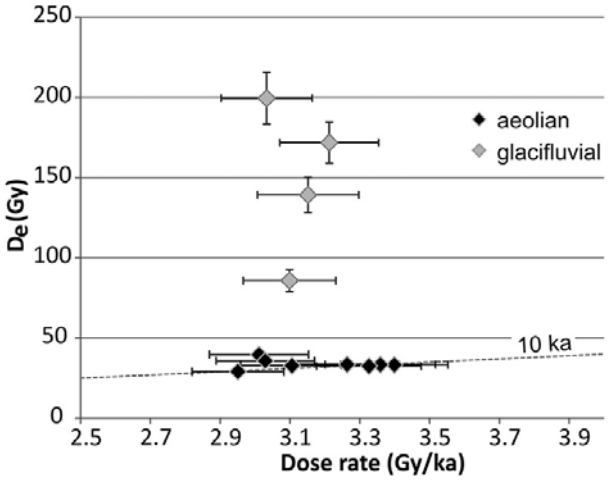

Fig. 4. In this plot of equivalent dose vs dose rate, the aeolian samples fall along a line corresponding to 10 ka age. The glacifluvial samples do not show such a relationship, which suggests that they are incompletely bleached. The two young aeolian samples are not included in this plot.

5.3. Timing of aeolian activity

The two OSL ages from a dune at Jømna are older (13.2-12.4 ±0.8 ka) than the ages from the Starmoen dunes (10.6-9.8 ±0.6 ka, Table S1), and older than the deposition of the underlying

glacifluvial sediments (see 5.2 above), which makes them unlikely to be true. The broad dose distribution, discussed above, does not necessarily explain the apparent age overestimation, and we do not have positive evidence of incomplete bleaching. Instead, a possible cause may be underestimation of the dose rate, since there appears to be disequilibrium in the ^{238}U-series for these samples (^{238}U:^{226}Ra activity ratio ≠ 1; Table S5). Based on data available, we cannot quantify the effect but a higher dose rate would make the ages somewhat younger.

The aeolian deposition likely started as soon as the main meltwater flow into the Jømna valley was cut off when the ice margin left Elverum and the jökulhlaup ceased, causing the river beds to largely dry out. Thus the jökulhlaup at ~10.5-10 cal. ka BP (Longva, 1994; see 2) should provide a maximum age for the aeolian deposition. The OSL ages of the dunes at Starmoen 1 and 3 overlap with the jökulhlaup age, which suggests that aeolian activity started immediately after the ice margin retreated. Our OSL ages from the Starmoen dune field thus confirm the general belief that most Scandinavian inland dune fields formed right after deglaciation, when sand was abundant, vegetation was scarce and winds were strong (Högbom, 1923; Hörner, 1927; Holtedahl, 1953). Starmoen now adds to the growing number of absolutely dated inland aeolian records in Sweden and Norway that will allow us to better explore this underused palaeoenvironmental archive.

The Starmoen dune field does, however, differ from other dated sites in one aspect: the duration of the dune building phase, which at sites in Sweden and Finland has been shown to last a few thousand years (Käyhkö et al., 1999; Alexanderson and Fabel, 2015). At Starmoen, the seven OSL ages from the Starmoen dunes overlap within one sigma (Fig. 2, Table S1), which implies a very brief period with dune formation. This is supported by sedimentological and geophysical data from the dunes, showing only minor reworking within dunes and limited dune migration (Henriksen et al., in prep.; Alexanderson and Henriksen, 2014). Based on the OSL ages and the ^{14}C age of the flood deposits, the timing of the event seems to be limited to between 10.5 cal. ka BP (the maximum age limit of the ^{14}C age of the flood deposits) and 9.8±0.6 ka (youngest OSL age). From geomorphological and climatological reasoning, Klemsdal (2010) suggests a duration of the event as short as 50-100 years, which we cannot resolve with current dating techniques.

Aeolian processes are considered among the most efficient in zeroing of the luminescence signal, even in glacial environments (Fuchs and Owen, 2008). However, the $D_e(t)$-plots of the aeolian samples (Fig. S7; cf. Bailey, 2003), although largely horisontal, show a slight rising trend towards the end, somewhat more pronounced for the basal aeolian sediments that directly overlie the glacifluvial sediments than for upper aeolian sediments. This may suggest that that during initial aeolian deposition, reworking was not sufficient to completely reset the slow signal components, which take longer to bleach than the faster components (Singarayer et al., 2005). Nevertheless, the fast signal

component appears fully bleached despite the brevity of the event and the limited reworking and aeolian influence on the grains as shown by sedimentology (Henriksen et al., in prep.).

The cessation of aeolian activity and the stabilisation of the dunes at Starmoen is suggested by Klemsdal (2010) to be due to improved climate and vegetation immigration. We also find this likely and agree with his interpretation, as birch followed by pine immigrated rapidly into the area and around 9000 cal. ka b2k the climate became warmer and wetter (Sørensen and Høeg, 2004).

During fieldwork, we hypothesised that the thin sand bed at Starmoen 4, between two soils in the area affected by the forest fire in 1976, was aeolian sand re-activated after the forest fire. However, the OSL age (770±110 years, Fig. 2) does not support this. The age is older than AD 1976, and rather suggests deposition in the 12th to 14th century. We therefore seem to record an earlier event instead of the 1976 forest fire. The cause and extent of this event is so far unknown.

The modern dune at the sand pit (Starmoen 2) migrates over small six-year-old pines (Fig. 2), which were established prior to the dune, or very early in its existence. The dune should thus be about or younger than six years, but its OSL age is 14±5 years (sample 13018). Most aliquots show no signal above background and provide equivalent doses consistent with zero within error, suggesting that the age should not be taken at face value but rather be considered as 'modern age' only. This nevertheless shows that the aeolian material in this area can be bleached.

6. Conclusions

Aeolian activity began in the Jømna valley (SE Norway) immediately after the ice sheet had retreated from Elverum and large meltwater input had ceased. OSL ages show that the dunes in the Starmoen dune field were built during a very short period ~10 ka ago, most likely within a few hundred years. These ages confirm the hypothesis that Scandinavian inland dune fields are deglacial in age, and provide the so far best absolute age constraints on the deglaciation in the Elverum area. There does not appear to have been any significant reworking of aeolian sand here during the Holocene, but a thin sand bed dated to the 12th-14th centuries may indicate a historical sand drift event. A small active dune at a sand pit gave a modern OSL age. The OSL ages of the underlying glacifluvial sediments are not reliable due to incomplete bleaching and to poor luminescence characteristics, and only provide maximum ages (<28 ka) of the deposition.

7. Acknowledgements

This study was carried out with financial support from the Crafoord Foundation and the Norwegian University of Life Sciences/Research Council of Norway ('småforsk'). Lodging during fieldwork as well as local information was provided by the Starmoen Flight Club and its members. Thanks also to Rolf

Sørensen and Jon Landvik for valuable discussions, and to the anonymous reviewer who constructively commented on the manuscript.

8. References

Alexanderson, H., Murray, A.S., 2012. Problems and potential of OSL dating Weichselian and Holocene sediments in Sweden. Quaternary Science Reviews 44: 37-50.

Alexanderson, H., Henriksen, M., 2014. A short-lived aeolian event during the Early Holocene in southern Norway In, 14th International Conference on Luminescence and Electron Spin Resonance Dating. Université du Québec à Montréal, p. 1. Abstract at http://www.led2014.uqam.ca/images/circulaires/Book%20of%20abstract%20Internet.pdf; poster at https://lup.lub.lu.se/search/publication/4925408.

Alexanderson, H., Fabel, D., 2015. Holocene chronology of the Brattforsheden delta and inland dune field, SW Sweden. Geochronometria 42: 1-16.

Arnold, L.J., Bailey, R.M., Tucker, G.E., 2007. Statistical treatment of fluvial dose distributions from southern Colorado arroyo deposits. Quaternary Geochronology 2 (1-4): 162-167.

Bailey, R.M., 2003. Paper I: The use of measurement-time dependent single-aliquot equivalent-dose estimates from quartz in the identification of incomplete signal resetting. Radiation Measurements 37 (6): 673-683.

Banerjee, D., Murray, A.S., Bøtter-Jensen, L., Lang, A., 2001. Equivalent dose estimation using a single aliquot of polymineral fine grains. Radiation Measurements 33: 73-94.

Bargel, T.H., 1983. Elverum. Beskrivelse til kvartærgeologisk kart 2016 IV - M 1 : 50 000. Geological Survey of Norway. 376. (In Norwegian.)

Bateman, M.D., 2008. Luminescence dating of periglacial sediments and structures. Boreas 37 (4): 574-588.

Bergqvist, E., 1981. Svenska inlandsdyner, Översikt och förslag till dynreservat. Statens naturvårdsverk. Rapport PM 1412. (In Swedish.)

Duller, G.A.T., 2003. Distinguishing quartz and feldspar in single grain luminescence measurements. Radiation Measurements 37 (2): 161-165.

Fitzsimmons, K.E., 2011. An assessment of the luminescence sensitivity of Australian quartz with respect to sediment history. Geochronometria 38 (3): 199-208.

Fuchs, M., Owen, L.A., 2008. Luminescence dating of glacial and associated sediments: review, recommendations and future directions. Boreas 37 (4): 636-659.

Galbraith, R.F., Roberts, R.G., Laslett, G.M., Yoshida, H., Olley, J.M., 1999. Optical dating of single and multiple grains of quartz from Jinmium rock shelter, northern Australia. Part I: experimental design and statistical models. Archaeometry 41 (2): 339-364.

Henriksen, M., Alexanderson, H., Jakobsen, L.V., Kalińska-Nartiša, E., in prep. Sedimentology and sediment architecture of inland dunes in SE Norway.

Holtedahl, O., 1953. Norges geologi. Aschehoug, Oslo. (In Norwegian.)

Högbom, I., 1923. Ancient Inland Dunes of Northern and Middle Europe. Geografiska Annaler 5: 113-243.

Hörner, N.G., 1927. Brattforsheden ett värmländskt randdeltekomplex och dess dyner. Geological Survey of Sweden. SGU C342. (In Swedish with English summary.)

Jeong, G.Y., Choi, J.-H., 2012. Variations in quartz OSL components with lithology, weathering and transportation. Quaternary Geochronology 10: 320-326.

Klemsdal, T., 1969. Eolian Forms in Parts of Norway. Norsk Geografisk Tidsskrift 23 (2): 49-66.

Klemsdal, T., 2010. The eolian landforms and sediment in the valley of River Jømna, east of Elverum, south-east Norway. Norsk Geografisk Tidsskrift 64 (2): 94-104.

Käyhkö, J.A., Worsley, P., Pye, K., Clarke, M.L., 1999. A revised chronology for aeolian activity in subarctic Fennoscandia during the Holocene. The Holocene 9 (2): 195-205.

Lancaster, N., 2008. Desert dune dynamics and development: insights from luminescence dating. Boreas 37 (4): 559-573.

Lepper, K., Larsen, N.A., McKeever, S.W.S., 2000. Equivalent dose distribution analysis of Holocene eolian and fluvial quartz sands from Central Oklahoma. Radiation Measurements 32 (5-6): 603-608.

Lomax, J., Hilgers, A., Twidale, C.R., Bourne, J.A., Radtke, U., 2007. Treatment of broad palaeodose distributions in OSL dating of dune sands from the western Murray Basin, South Australia. Quaternary Geochronology 2 (1-4): 51-56.

Longva, O., 1994. Flood Deposits and Erosional Features from the Catastrophic Drainage of Preboreal Glacial Lake Nedre Glåmsjø, SE Norway. Department of Geology, University of Bergen. PhD thesis p.

Longva, O., Thoresen, M.K., 1991. Iceberg scours, iceberg gravity craters and current erosion marks from a gigantic Preboreal flood in southeastern Norway. Boreas 20: 47-62.

Lundqvist, J., Mejdahl, V., 1995. Luminescence dating of the deglaciation in northern Sweden. Quaternary International 28: 193-197.

Murray, A.S., Wintle, A.G., 2000. Luminescence dating of quartz using an improved single-aliquot regenerative-dose protocol. Radiation Measurements 32 (1): 57-73.

Murray, A.S., Wintle, A.G., 2003. The single aliquot regenerative dose protocol: potential for improvements in reliability. Radiation Measurements 37 (4-5): 377-381.

Murray, A.S., Marten, R., Johnson, A., Martin, P., 1987. Analysis for naturally occurring radionuclides at environmental concentrations by gamma spectrometry. Journal of Radioanalytical and Nuclear Chemistry Articles 115: 263-288.

Olley, J., Caitcheon, G., Murray, A., 1998. The distribution of apparent dose as determined by optically stimulated luminescence in small aliquots of fluvial quartz: implications for dating young sediments. Quaternary Science Reviews 17 (11): 1033-1040.

Pietsch, T.J., Olley, J.M., Nanson, G.C., 2008. Fluvial transport as a natural luminescence sensitiser of quartz. Quaternary Geochronology 3 (4): 365-376.

Prescott, J.R., Hutton, J.T., 1994. Cosmic ray contributions to dose rates for luminescence and ESR dating: large depths and long-term time variations. Radiation Measurements 23: 497-500.

Seppälä, M., 1972. Location, Morphology and Orientation of Inland Dunes in Northern Sweden. Geografiska Annaler. Series A, Physical Geography 54 (2): 85-104.

Singarayer, J.S., Bailey, R.M., Ward, S., Stokes, S., 2005. Assessing the completeness of optical resetting of quartz OSL in the natural environment. Radiation Measurements 40 (1): 13-25.

Sørensen, R., Høeg, H.I., 2004. Tidlig jordbruk i Østerdalene In: Vesseltun, I., Ellingsberg, A., Syrstad, O., Olsen, O.B., Aas jr., E., Øygard, G. and Lie, V. (Eds.), Jord og gjerning. Norsk Landbruksmuseum, pp. 31-48. (In Norwegian.)

Thrasher, I.M., Mauz, B., Chiverrell, R.C., Lang, A., 2009. Luminescence dating of glaciofluvial deposits: A review. Earth-Science Reviews 97 (1-4): 145-158.

Vandenberghe, D., Hossain, S.M., De Corte, F., van den Haute, P., 2003. Investigations on the origin of the equivalent dose distribution in a Dutch coversand. Radiation Measurements 37 (4–5): 433-439.

Wolfe, S.A., 2007. Dune fields - High Latitudes. In: Elias, S.A. (Ed.) Encyclopedia of Quaternary Science, 10.1016/B0-44-452747-8/00159-9. Elsevier, Oxford, pp. 599-607.

Supplementary material

Methods

Fourteen samples for luminescence dating were taken by hammering opaque plastic tubes into freshly cleaned sediment exposures during fieldwork in May 2013. The luminescence samples were kept dark and cool until opened under dark room conditions at the Lund Luminescence Laboratory at Lund University, Sweden. After wet-sieving to extract the 180-250 µm fraction, preparation included standard treatment with 10% HCl to remove carbonates, 10% H_2O_2 to remove any organic material and density separation at 2.62 g/cm (LST Fastfloat). The quartz separate was then treated with 38% HF to remove remaining impurities and to etch the outer surface of the grains, and finally with 10% HCl to clean out any fluorides.

Water content was measured on separate 100 cm^3 subsamples, and the field capacity, the water content at time of sampling and the saturated (maximum) water content were determined. Based on the location of the samples, in quickly drained sediments above the groundwater table, we chose to use the water content at time of sampling as the average water content since deposition, increased by 10% to account for any drying that may have taken place between sampling (May) and analysis (August).

The Risø TL/OSL reader model DA-20 reader used for measurement was equipped with a $^{90}Sr/^{90}Y$ beta radiation source (dose rate 0.16 Gy/s), blue (470±30 nm; ~50 mW/cm^2) and infrared (880 nm, w100 mW/cm^2) light sources. Detection was through 7 mm of U340 glass filter. The equivalent dose (D_e) was calculated by integrating the OSL signal from channels 1 to 5 (the first 0.8 s), subtracting an early background (channels 6 to 10, the next 0.8 s), and using exponential curve fitting in Risø Analyst v. 3.24. For one sample (Lund 13021), channels 1-10 and 11-20 were used instead as it gave better dose recovery.

IR-tests (Duller, 2003) were used to check for feldspar contamination of the quartz samples. Most samples showed infrared/blue ratios of <5% and insignificant feldspar contamination. However, significant feldspar contamination was observed for three samples. A few aliquots from samples 13021 and 13023 had ratios >10%, and a SAR-protocol including an IR-check was used to identify any feldspar-contaminated aliquots (Table S2). In sample 13013, several aliquots had IR/blue ratios >20% and a post-IR blue protocol was adopted (Banerjee et al., 2001). The equivalent dose showed only a weak relationship with IR/blue ratio (R^2=0.02), but any aliquots with a ratio >10% were nonetheless rejected.

Tables and figures

Table S1. OSL data from the Starmoen area.

Lab no.	Site	Altitude (m a.s.l.)	Depth (m)	Sediment	Age (ka)	Dose (Gy)	n acc./total [1]	Aliquot size [2]	Dose rate (Gy/ka)	w.c. (%)	Sensitivity ($cts \cdot s^{-1} \cdot Gy^{-1}$)
Lund 13013	Starmoen 1	202	3.7	glacifluvial	27.6 ± 2.7	85.6 ± 7.3	21/27	large	3.10 ± 0.13	13	174 ± 49
					29.0 ± 2.3	90.0 ± 5.6	38/93	small	3.10 ± 0.13	13	
					14.2 ± 1.5	44.0 ± 4.0	p=0.016	MAM3	3.10 ± 0.13	13	
Lund 13014	Starmoen 1	203	3.0	aeolian	10.3 ± 0.7	33.7 ± 1.6	20/27	large	3.26 ± 0.15	5	104 ± 27
Lund 13015	Starmoen 1	203	2.8	aeolian	10.6 ± 0.6	32.9 ± 0.7	25/27	large	3.11 ± 0.15	3	184 ± 46
					9.6 ± 0.5	29.7 ± 0.5	51/96	small	3.11 ± 0.15	3	
					9.8 ± 0.8	30.5 ± 1.7	p=0.7	MAM3	3.11 ± 0.15	3	
Lund 13016	Starmoen 1	204	1.3	aeolian	9.8 ± 0.5	33.4 ± 0.8	28/30	large	3.40 ± 0.15	5	179 ± 88
Lund 13017	Starmoen 1	205	0.7	aeolian	10.0 ± 0.5	33.5 ± 0.7	26/27	large	3.36 ± 0.16	4	166 ± 38
Lund 13018	Starmoen 2	210	0.3	aeolian	0.014 ± 0.005	0.05 ± 0.02	16/24	large	3.62 ± 0.17	6	1398 ± 1026
Lund 13019	Starmoen 3	207	4.2	aeolian	9.9 ± 0.5	29.2 ± 0.7	29/42	large	2.95 ± 0.13	11	169 ± 38
Lund 13020	Starmoen 3	210	1.2	aeolian	9.8 ± 0.6	32.7 ± 1.1	26/27	large	3.33 ± 0.15	6	113 ± 18
Lund 13021	Jømna	189	3.0	glacifluvial	43.5 ± 4.2	137.1 ± 11.5	35/39	large	3.15 ± 0.15	4	629 ± 199
					44.5 ± 4.1	140.3 ± 10.8	34/96	small	3.15 ± 0.15	4	
					25.2 ± 3.1	79.5 ± 8.8	p=0.05	MAM3	3.15 ± 0.15	4	
Lund 13022	Jømna	190	1.9	aeolian	13.2 ± 0.8	39.8 ± 1.3	26/33	large	3.01 ± 0.14	7	167 ± 40
					14.7 ± 0.9	44.1 ± 1.6	41/96	small	3.01 ± 0.14	7	
					11.5 ± 1.2	34.5 ± 3.1	p=0.02	MAM3	3.01 ± 0.14	7	
Lund 13023	Jømna	191	1.0	aeolian	12.4 ± 0.7	37.5 ± 0.8	22/26	large	3.03 ± 0.14	6	593 ± 177
Lund 13024	Hornmoen bruk	212	2.0	glacifluvial	65.8 ± 6.2	199.6 ± 16.2	23/30	large	3.03 ± 0.13	11	659 ± 189
Lund 13025	Hornmoen bruk	211	1.2	glacifluvial	53.5 ± 4.8	171.9 ± 12.8	23/33	large	3.21 ± 0.14	8	944 ± 241
Lund 13026	Starmoen 4	213	0.1	aeolian	0.77 ± 0.11	1.7 ± 0.2	27/27	large	2.16 ± 0.11	10	2334 ± 1256

[1] number of aliquots that were accepted of the total number measured. For the MAM3, the p-value is given here

[2] large aliquots are 8 mm in diameter, small aliquots are 2 mm, and MAM3 represents 2-mm aliquots for which the age has been calculated with the three-parameter minimum age model (Galbraith et al., 1999) and using a macro designed by Sebastien Huot

Table S2. Single-aliquot regeneration (SAR) protocols with the settings given below were used in this study.

Sample	Preheat	Cutheat	Test dose (Gy)	Lightsource/s
13013	260°	240°	16-20	post-IR blue
13014-17, 19-20, 22	260°	240°	16	blue
13018	200°	180°	1.6-3.2	blue
13021	180°	160°	20	blue + IR-check
13023	260°	240°	16	blue + IR-check
13024-25	220°	200°	20	blue
13026	180°	160°	1.6	blue

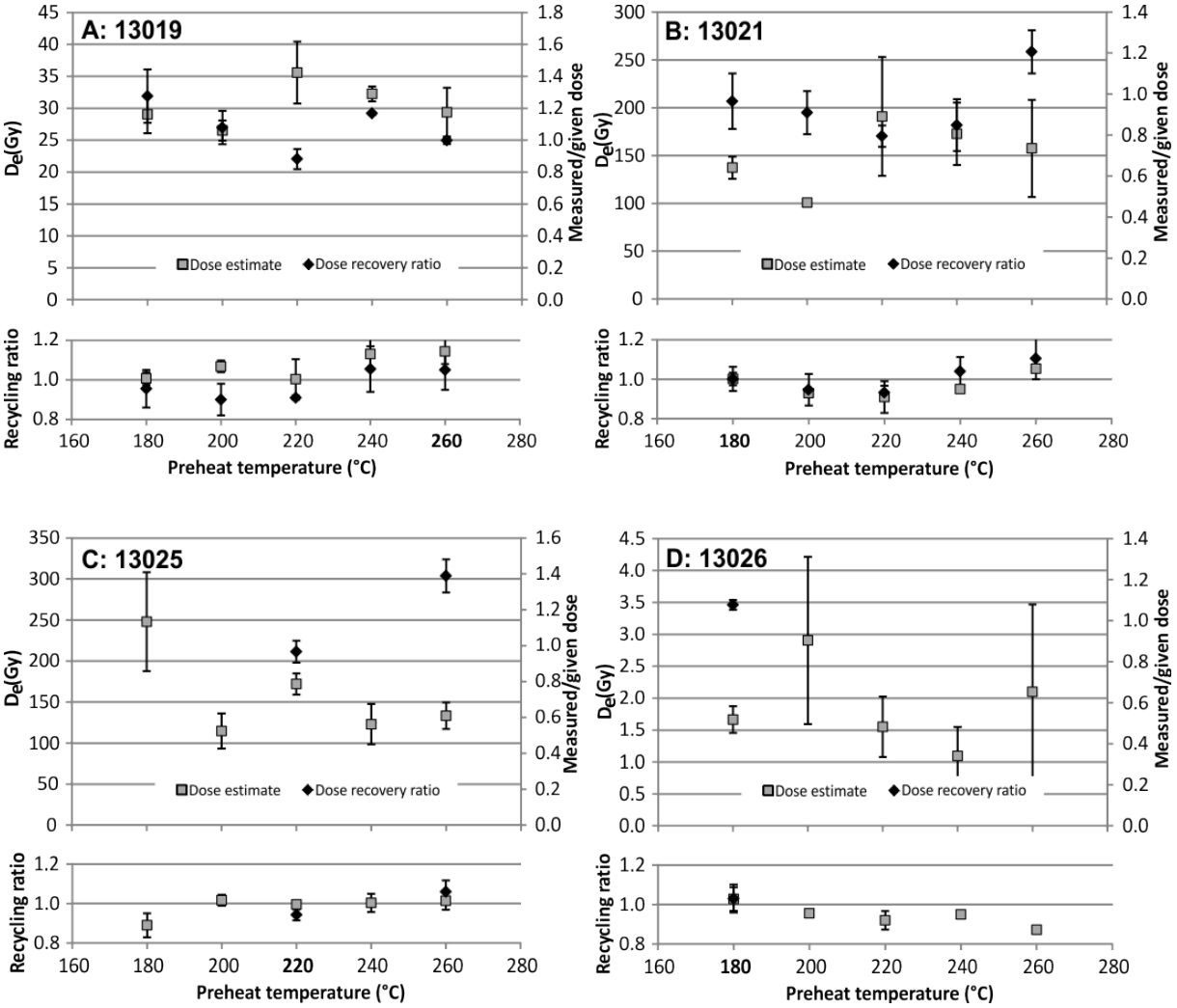

Fig. S3. Preheat plateau tests for four representative samples, two aeolian and two glacifluvial from the two areas Starmoen and Jømna. (A) sample Lund-13019, (B) Lund-13021, (C) Lund-13025 and (D) Lund-13026. Three aliquots per temperature setting were measured for each sample, and in these plots the mean with related standard error is shown. Selected preheat temperatures are in bold.

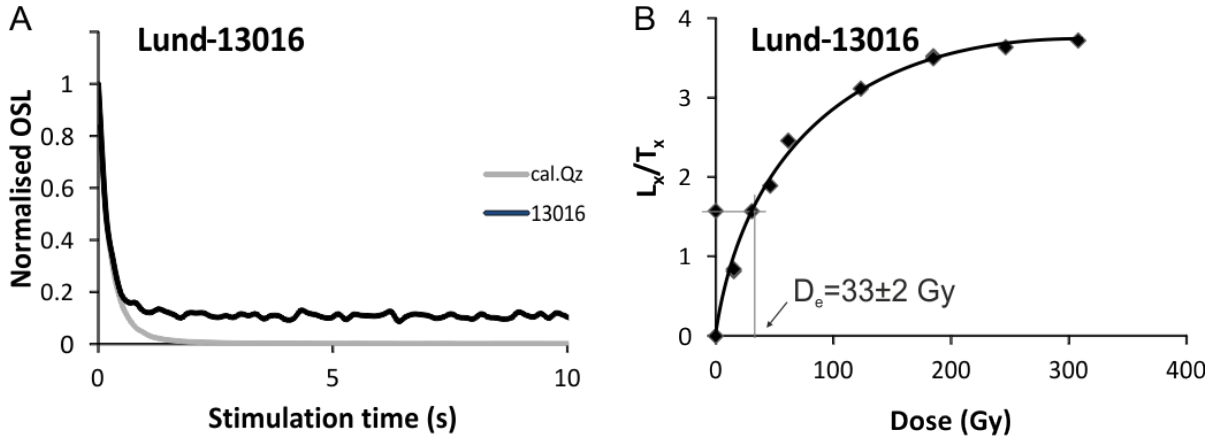

Fig. S4. Example of decay curve (A) and dose-response curve (B) from the aeolian sample Lund-13016 from Starmoen 1. The comparison in (A) with the luminescence signal from Risø calibration quartz shows that the signal from the Starmoen quartz is dominated by a fast component, but has a lower signal to noise ratio than the calibration quartz.

Table S5. Summary of radionuclide specific activities measured with high-resolution gamma spectrometry for the samples from the Starmoen area. Beta and gamma dose rates refer to dry material; for water contents and final dose rates see Table S1.

Lab no.	Site	^{238}U (Bq/kg)	^{226}Ra (Bq/kg)	^{232}Th (Bq/kg)	^{40}K (Bq/kg)	Gamma (Gy/ka)	Beta (Gy/ka)
Lund 13013	Starmoen 1	50 ± 7	22 ± 0.6	21 ± 0.5	830 ± 16	1.06 ± 0.02	2.40 ± 0.05
Lund 13014	Starmoen 1	20 ± 6	19 ± 0.5	20 ± 0.5	851 ± 16	1.04 ± 0.02	2.30 ± 0.04
Lund 13015	Starmoen 1	27 ± 8	15 ± 0.6	16 ± 0.6	803 ± 18	0.93 ± 0.02	2.17 ± 0.05
Lund 13016	Starmoen 1	20 ± 6	22 ± 0.5	22 ± 0.6	866 ± 16	1.10 ± 0.02	2.37 ± 0.04
Lund 13017	Starmoen 1	8 ± 11	20 ± 0.8	21 ± 1.0	866 ± 20	1.06 ± 0.02	2.30 ± 0.06
Lund 13018	Starmoen 2	72 ± 12	25 ± 1.0	23 ± 0.9	848 ± 22	1.13 ± 0.03	2.56 ± 0.07
Lund 13019	Starmoen 3	23 ± 9	21 ± 0.7	21 ± 0.8	796 ± 17	1.02 ± 0.02	2.21 ± 0.06
Lund 13020	Starmoen 3	21 ± 7	22 ± 0.6	23 ± 0.6	838 ± 16	1.09 ± 0.02	2.31 ± 0.05
Lund 13021	Jømna	16 ± 5	22 ± 0.5	24 ± 0.6	772 ± 14	1.04 ± 0.02	2.14 ± 0.04
Lund 13022	Jømna	9 ± 11	22 ± 0.9	19 ± 1.0	795 ± 22	1.00 ± 0.03	2.13 ± 0.07
Lund 13023	Jømna	9 ± 9	17 ± 0.8	18 ± 0.9	792 ± 20	0.96 ± 0.02	2.10 ± 0.06
Lund 13024	Hornmoen bruk	48 ± 7	23 ± 0.6	23 ± 0.5	767 ± 15	1.03 ± 0.02	2.26 ± 0.05
Lund 13025	Hornmoen bruk	19 ± 6	22 ± 0.5	23 ± 0.6	824 ± 16	1.08 ± 0.02	2.27 ± 0.05
Lund 13026	Starmoen 4[a]	-13 ± 15	16 ± 1.0	14 ± 0.9	539 ± 19	0.70 ± 0.02	1.39 ± 0.08

[a] A negative ^{238}U activity is not realistic but the value is >0 within error. The sample has been measured twice, with similar results. If the mean dose rate of the source sediments (the older aeolian sediments at Starmoen) is assumed, the resulting age instead becomes 520±70 yr.

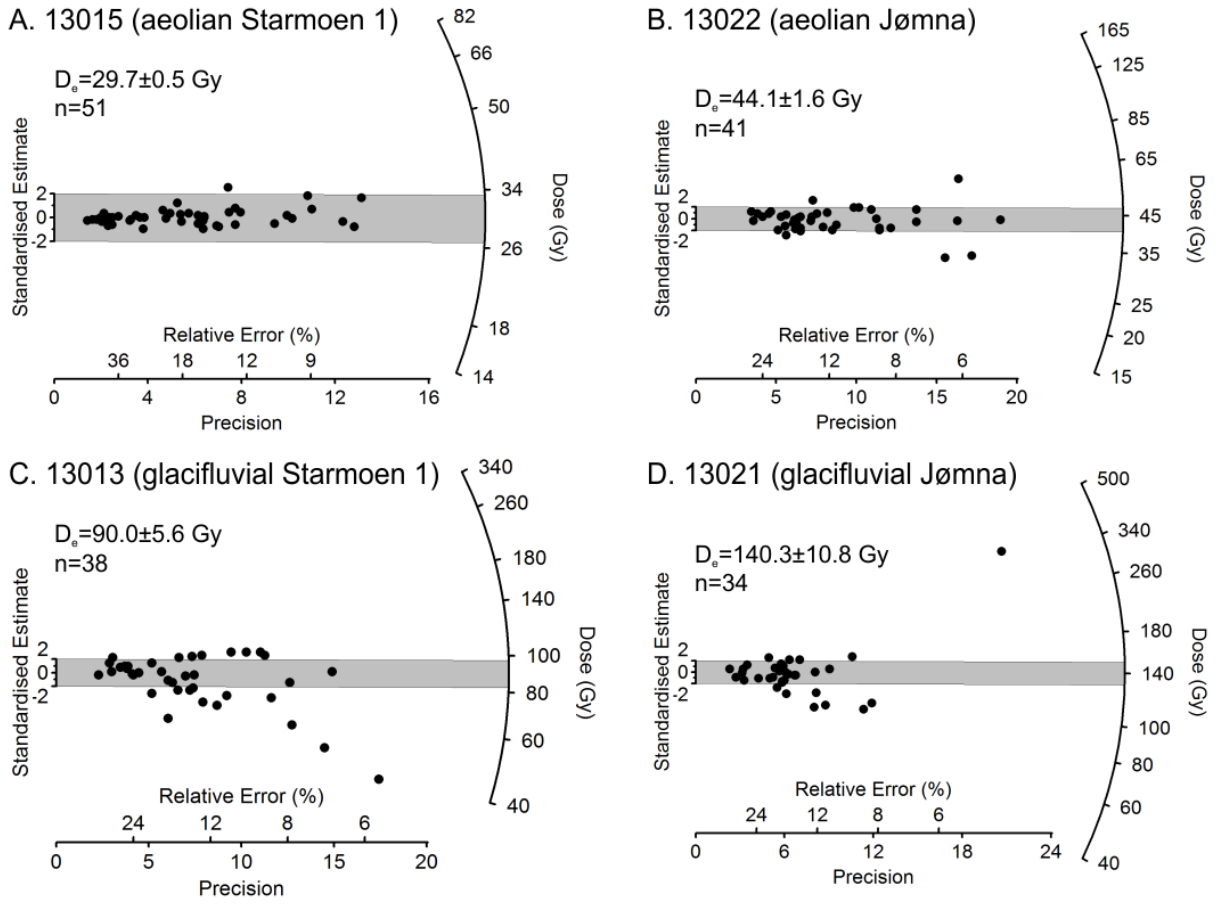

S 6. Radial plots of dose distributions from small aliquots of two aeolian and two glacifluvial samples from the sites Starmoen 1 and Jømna. The grey shading shows the spread (two sigma) of the distributions. A. Lund-13015 from aeolian sand, B. Lund-13022 from aeolian sand, C. Lund-13013 from glacifluvial sand and D. Lund-13021 from glacifluvial sand.

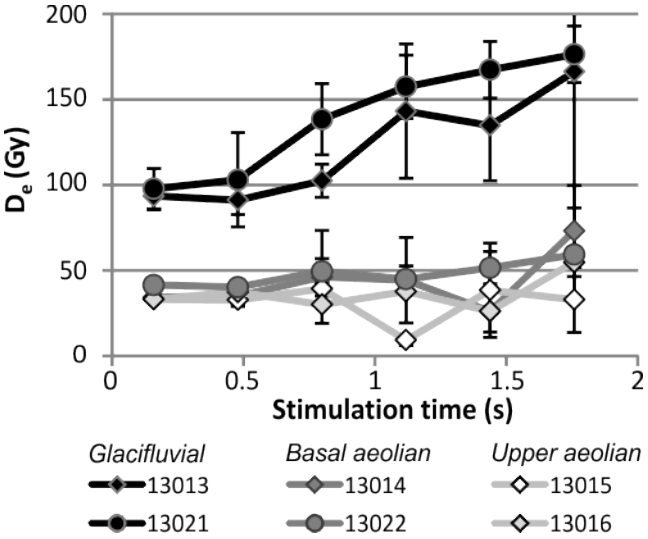

Fig. S 7. Plot with D_e as a function of stimulation time for samples from Starmoen (diamonds) and Jømna (circles); the median value of 15 aliquots per sample is plotted and the vertical bars represent the standard error. The dose of the glacifluvial samples show an increase with stimulation time, indicating that they are incompletely bleached. The aeolian samples show a more horisontal trend, but particularly for the basal aeolian sediments there is a slight rising trend that may suggest that the slow signal components are not completely bleached.